

Supplementary Information for
Substituted ferrocenes and iodine as synergistic thermoelectrochemical
heat harvesting redox couples in ionic liquids

E.H.B. Anari,^a M. Romano,^b W.X. Teh,^a J.J. Black,^a E. Jiang,^a J. Chen,^b T.Q. To,^a J.

Panchompoo^a and L. Aldous^{a*}

^{a.} *School of Chemistry, UNSW Australia, Sydney, NSW 2052, Australia*

^{b.} *Intelligent Polymer Research Institute, Innovation Campus, University of Wollongong,
Wollongong, NSW 2522, Australia*

* Corresponding author; l.alldous@unsw.edu.au

1. Synthesis of the substituted ferrocenes

Acylferrocenes and alkylferrocenes such as acetyl ferrocene (AcFc), ethyl ferrocene (EtFc), 1,1'-dibutanoylferrocene (DiBoylFc) and 1,1'-dibutylferrocene (DiBuFc) were synthesised from ferrocene ($\text{Fe}(\text{C}_5\text{H}_5)_2$, 99%, Strem Chemicals Inc.) *via* a Friedel-Crafts acylation reaction, followed by a chemical reduction/alkylation process.¹ In this work, monoacylation and diacylation of ferrocene were performed using the phosphoric acid (H_3PO_4 , $\geq 99.99\%$, Sigma Aldrich) and aluminium chloride (AlCl_3 , $\geq 99\%$, Fluka) catalysed methods, respectively.²

Acetyl ferrocene (AcFc) was first synthesised *via* Friedel-Crafts acylation by dissolving a weighed stoichiometric amount of ferrocene in acetic anhydride in the presence of phosphoric acid as a catalyst.² The reaction mixture was stirred at 25 °C in the water bath for a period of time. Then, water was added to this mixture, and the corresponding solution was neutralised

by dropwise addition of sodium bicarbonate (NaHCO_3). The reaction mixture was further stirred at 25 °C until the colour of the organic layer changed from yellow to red, indicating that the acetylated ferrocene was successfully formed by this acetylation reaction. The red organic layer was next extracted using a separation funnel, and acetic anhydride was removed over a rotavapor to afford crude acetyl ferrocene as a clear orangish-red liquid, which was further purified using column chromatography with gradient ethyl acetate : hexane elution. The ^1H NMR spectrum of resulting product shows four proton signals at δ of 2.4 ppm (3H, singlet), 4.2 ppm (5H, Singlet), 4.5 (2H, triplet), 4.8 (2H, triplet), corresponding to ^1H NMR spectrum of acetyl ferrocene.

Subsequently, the acetyl ferrocene was reduced to ethylferrocene (EtFc) by the Clemensen reduction method.³ A short silica column follow by distillation yielded pure ethylferrocene. Three proton signals of EtFc could be observed at δ of 1.2 ppm (3H, triplet), 2.4 ppm (2H, quartet) and 4.0 ppm (9H, broad), confirming product identity and purity.

Dibutanoylferrocene (DiBoylFc) was next synthesised by mixing ferrocene and butyrylchloride in a ratio of 1:2 in dichloromethane (DCM) in the presence of 2 eq. aluminium chloride (AlCl_3). The reaction mixture was stirred at room temperature under nitrogen for *ca.* 36 h. After this time, water was added to the reaction mixture in an ice bath before the organic layer was extracted, washed extensively with water and dried over anhydrous magnesium sulfate (MgSO_4). Dichloromethane was then removed over a rotavapor to obtain crude 1,1-dibuanoylferrocene (DiBoyllFc) as a reddish-brown solid, which was further purified using column chromatography with gradient ethyl acetate : hexane

elution. The ^1H NMR spectrum of DiBoylFc shows five signals at δ of 0.95 ppm (6H, triplet), 1.39 ppm (4H, quartet), 1.52 ppm (4H, quartet), 2.36 ppm (4H, triplet) and 4.00 ppm (8H, singlet), corresponding to ^1H NMR spectrum of dibutyryl ferrocene.

Dibutylferrocene (DiBuFc) was subsequently prepared by reducing dibutyryl ferrocene with LiAlH_4 in the presence of AlCl_3 . Typically, *ca.* 1.5 g of lithium aluminium hydride (LiAlH_4 , 0.04 mol) were stirred in 50 mL of anhydrous diethyl ether (Et_2O) under nitrogen at room temperature. Then, *ca.* 5.3 g of aluminium chloride (AlCl_3 , 0.04 mol) was added dropwise to the LiAlH_4 solution, followed by gradual addition of *ca.* 5.0 g of dibutanoylferrocene (0.015 mol), resulting in the brownish orange solution. The reaction mixture was then heated up to 30 °C with vigorous stirring under nitrogen for 2 h. After this time, the reaction was quenched with water in an ice bath and the organic layer was extracted using a separatory funnel. Finally, diethyl ether was removed *in vacuo* to give dibutylferrocene ($\text{C}_{18}\text{H}_{26}\text{Fe}$) as a clear brownish orange liquid with a yield of *ca.* 91%. Thermogravimetric analysis highlighted the presence of a small quantity of non-volatile material, so distillation was performed using a Kugelrohr distillation apparatus (Buchi Glass Oven B-585 Kugelrohr). The ^1H NMR spectrum of the resulting dibutyl ferrocene shows five signals of protons at δ of 0.95 ppm (6H, triplet), 1.39 ppm (4H, quintet), 1.52 ppm (4H, quintet), 2.35 ppm (4H, triplet) and 4.00 ppm (8H, singlet), corresponding to ^1H NMR spectrum of dibutyl ferrocene.

2. Measurement of Seebeck coefficients and power discharge

Two measurement methods were utilised. Firstly a U-shaped thermocell (Fig. S1), as reported elsewhere.⁴

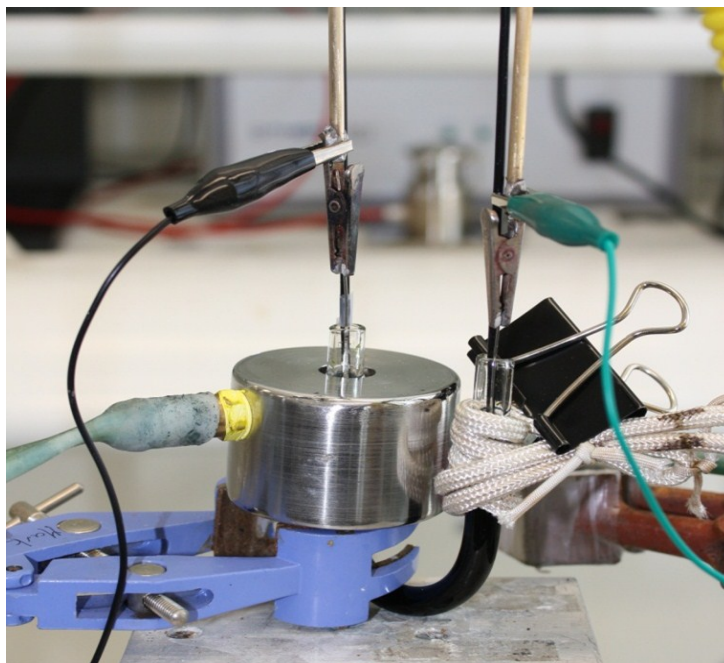


Fig. S1: U-shaped glass thermocell used for measurement of Seebeck coefficients. A black solution of ferrocene and iodine in the ionic liquid can clearly be observed.

T_{cold} was held at 20 °C using circulating liquid supplied by a Thermoline Scientific BL-30 refrigerated circulating bath. T_{hot} was increased in 10 °C increments through the use of an Omegalux Rope Heater FGR-060 connected to a TCA Control Box (accuracy ± 1 °C). Using the U-cell, a Seebeck coefficient of 1.42 mV/K was first obtained of 0.4 M $\text{K}_3\text{Fe}(\text{CN})_6/\text{K}_4\text{Fe}(\text{CN})_6$, which is in good agreement with literature (≈ 1.4 mV/K)⁵. This apparatus was then dried and employed for measurement of 30 mM of the various redox systems in [Emim][NTf₂].

Seebeck coefficients of various ionic liquid samples were measured using the setup as described above, by systematically heating – recording the steady state potential difference – heating further, and finally cooling down and recording the same data on the reverse. This was to ensure there was no hysteresis. The values were recorded in triplicate and the averages reported in the manuscript.

A second method employed a commercial battery casing, as reported elsewhere.⁶ Platinum-coated CR2032 battery casings were supplied by MTI Corporation (Richmond, CA, USA), which was supplied pre-sputter coated with platinum. CR2032 button cell battery cases are 20mm in diameter and 3.2mm deep, and can accommodate *ca.* 0.7mL electrolyte. The two metallic halves were crimped and a poly(propylene) rim on one half provided a hermetic seal, as well as electrical and thermal insulation between the two halves. Battery casings were crimped before use using a MSK-110 hydraulic crimping machine with a CR2032 crimping die, all supplied by MTI Corporation (Richmond, CA, USA).

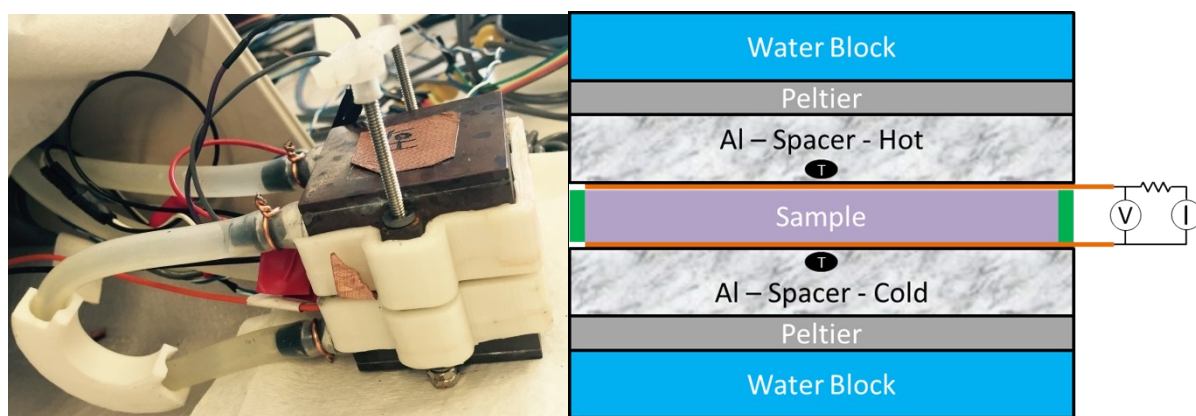


Fig. S2: A photo and a schematic to show how samples in CR2032 battery casings were heated and cooled to within 0.1°C accuracy. The black oval T indicates the location of the thermistors. Cells were always measured in the vertical orientation (photo is in parallel orientation)

The power output and potential differences were measured using a B2901A Precision Source/Measure Unit (SMU) that has the capability to source and measure both voltage and current. A B2901A Source/Measure unit from Keysight Technology (Australia) was used throughout. The Seebeck coefficient was determined by measuring the open circuit potential for the cell for 1500 seconds and then averaging the potential for the final 500 seconds. The initial 500 seconds were to allow the cell to reach the target temperature and stabilise. For power measurements, the SMU was then configured to draw current from the cell at various fixed current values, and the voltage was recorded. The voltage was measured for a period of 10 minutes, averaging the last 5 minutes to obtain the power characteristics for the cell. The raw data for the 30 mM [Fc][I₃] system is displayed below;

Seebeck coefficient determination:

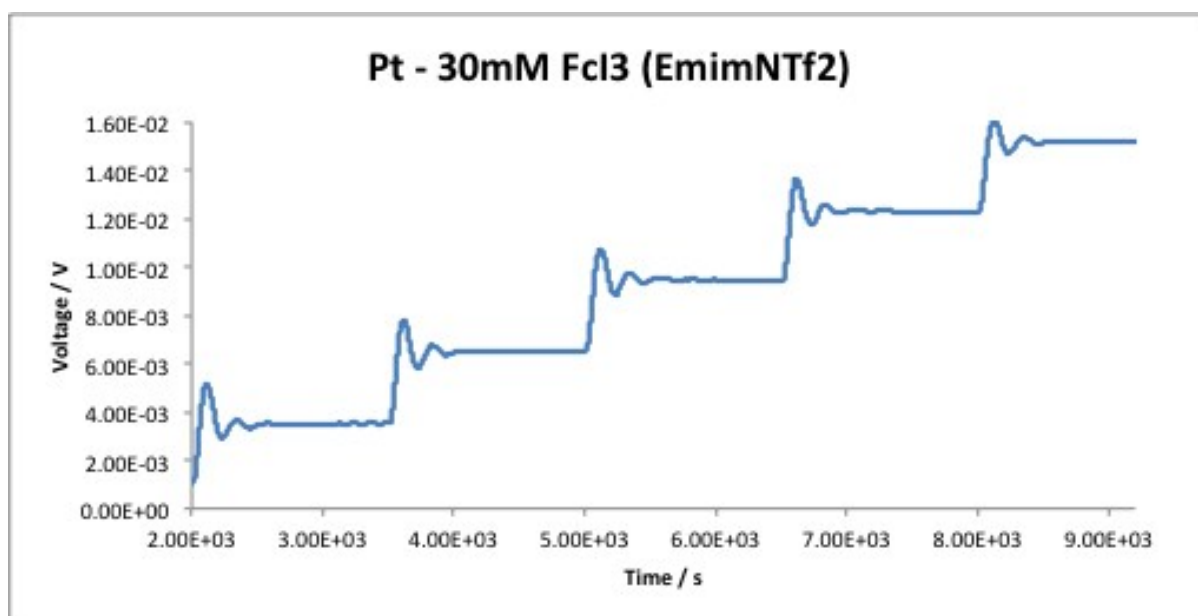


Fig. S3: Seebeck coefficient determination for 30 mM [Fc][I₃] in a Pt-coated CR2032 battery casing, where every 1,500 s the temperature difference was increased by 10 K (starts at $\Delta T = 10$ K)

Power discharge characteristics

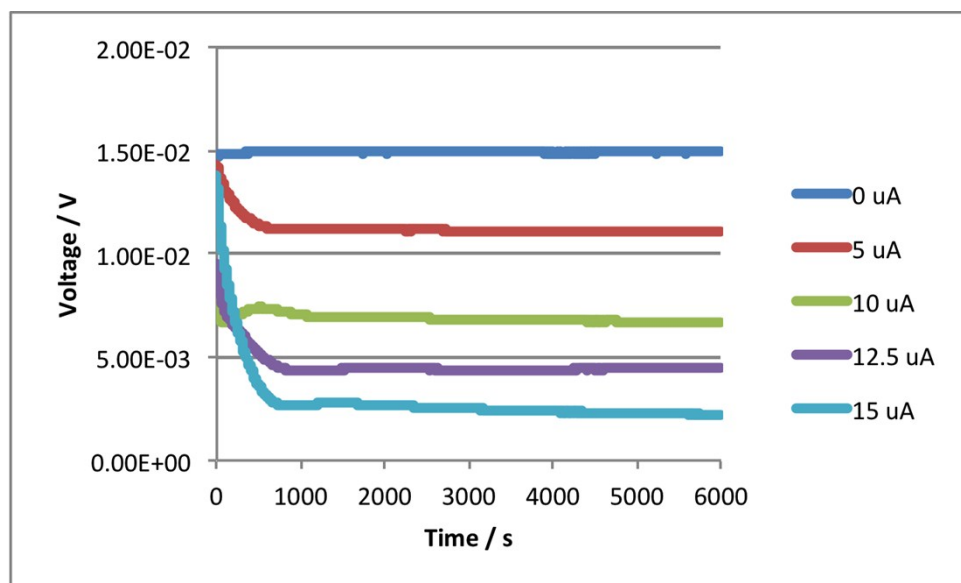


Fig. S4: Voltage required to sustain various discharge currents during discharge for 30 mM [Fc][I₃] in a Pt-coated CR2032 battery casing ($\Delta T = 50$ K). Note that fluctuations over longer periods of time in the voltage are largely due to the temperature variations; greater discharge currents resulted in longer temperature equilibration periods.

3. Cyclic voltammetry and use of Nernst equation to estimate ratio

Cyclic voltammetry was recorded using a μ Autolab PGSTAT 101 computer-controlled potentiostat (EcoChemie, Utrecht, The Netherlands) with Nova 1.10 software. Cyclic voltammetry (CV) was performed at room temperature at a scan rate of 50 mV s^{-1} (unless stated otherwise) using a standard three-electrode configuration employing (i) a Pt wire counter electrode, (ii) a 1.6 mm Pt working electrode and (iii) an Ag/Ag⁺ non-aqueous reference electrode kit (all from BASi, USA). The Ag/Ag⁺ non-aqueous reference electrode was filled with [Emim][NTf₂] containing *ca.* 10 mM AgNO₃ in order to provide a constant reference potential; this was subsequently corrected to the ferrocene/ferrocenium potential in the same ionic liquid on the day of use.

The following CVs display the relative oxidative potentials for the different ferrocene samples, and an example of how they compare with the iodide/triiodide/iodine redox couples.

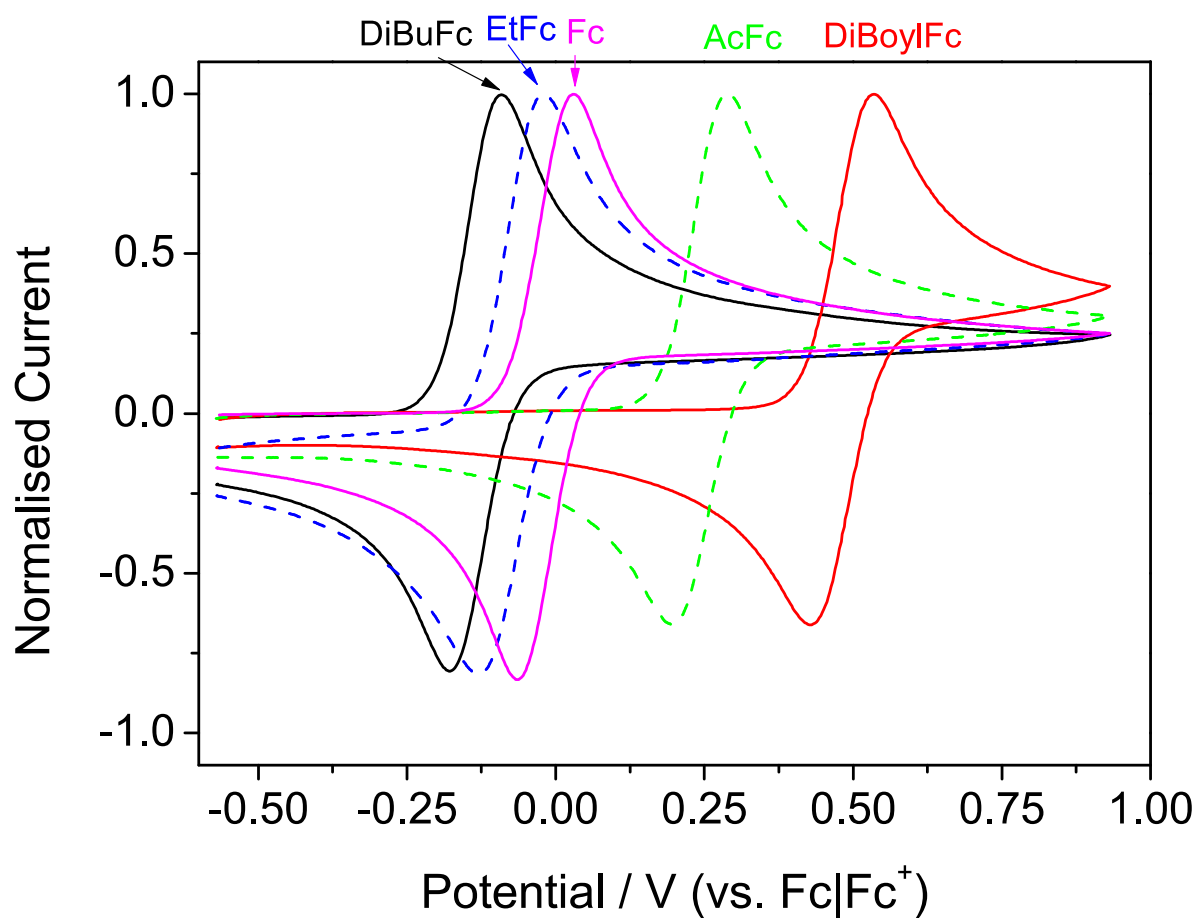


Fig. S5: Normalised CVs (with respect to the peak current of the oxidation feature) for the various ferrocene species investigated in this study. All refer to 30 mM of the ferrocene species dissolved in $[\text{Emim}][\text{NTf}_2]$, at a 1.6 mm Pt electrode, 50 mV s^{-1} , and corrected to the $\text{Fc}|\text{Fc}^+$ formal potential. Recorded at 293 K.

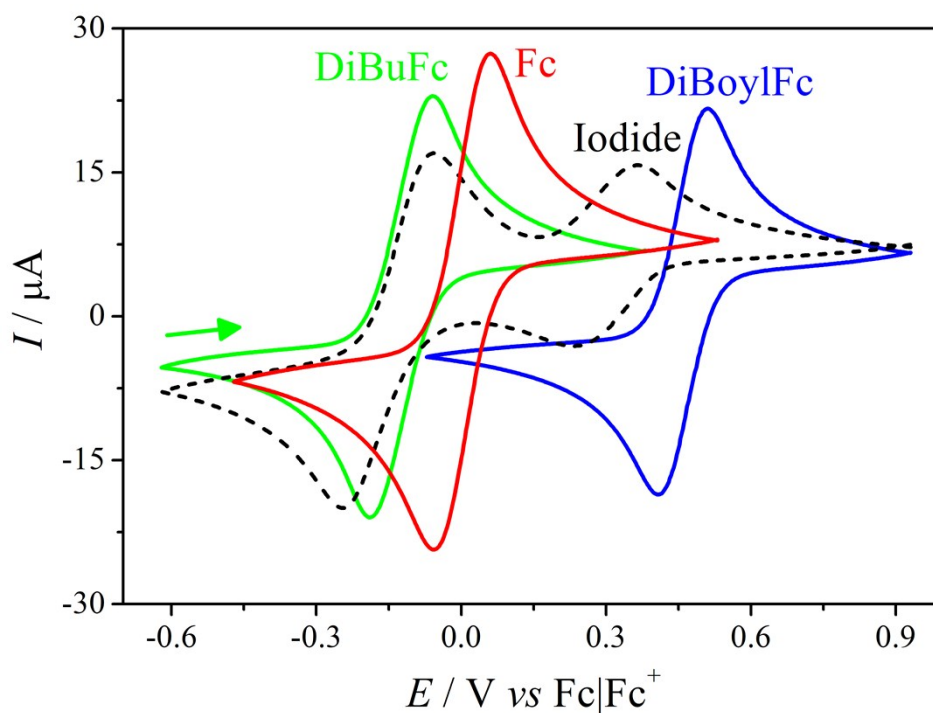
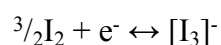


Fig. S6: CVs recorded for 30 mM DiBuFc, Fc and DiBoylFc in [Emim][NTf₂], as well as 45 mM [Emim]I (---). Scans recorded at a 1.6 mm Pt electrode, 50 mV s⁻¹, and corrected to the Fc | Fc⁺ formal potential. Recorded at 293 K.

From the cyclic voltammetry above, the following half-wave potentials were determined from $(E_{p,a} + E_{p,c})/2$, which are good estimates for the formal potential of the redox couples as all display reversible voltammetry.

	$E_{p/2} / \text{V (vs. Fc/Fc}^+)$
$\text{I}^-/[\text{I}_3]^-$	-0.15
$[\text{I}_3]^-/\text{I}_2$	0.30
DiBuFc	-0.12
EtFc	-0.06
Fc	0.00
AcFc	0.26
DiBoylFc	0.49

The difference in formal potentials is a good estimate for the effectiveness of compounds as, for example, oxidising agents. For simple 1 electron oxidants added in a stoichiometric (1:1 ratio) to a substrate, potential differences of 0 V, 0.118 V, 0.236 V and 0.354 V (at 293 K) predict oxidised:non-oxidised ratio's of 1:1, 1:10, 1:100 and 1:1000, respectively.⁷ This is derived from $\Delta E = -RT/nF \ln(Q)$. However, the Fc:I₂ reaction is not a 1:1 stoichiometry, as noted below;



In this system when ferrocene is mixed with iodine;

$$\Delta E = E_{p/2}(\text{ferrocene} \mid \text{ferrocenium}) - E_{p/2}(\text{triiodide} \mid \text{iodine}) = -RT/nF \ln(Q)$$

where $Q = ([\text{Fc}^+][\text{I}_3^-]/[\text{Fc}][\text{I}_2]^{3/2})$

If the ferrocene species, Fc, and iodine, I₂, are added in a 3:2 ratio then $[\text{I}_2] = \frac{2}{3}[\text{Fc}]$, and for every $[\text{Fc}^+]$ formed as a result a stoichiometric amount of $[\text{I}_3^-]$ will also be formed (*i.e.* $[\text{Fc}^+] = [\text{I}_3^-]$).

This allows us to simplify it to

$$\Delta E = RT/nF \ln ([\text{Fc}^+]^2/[\text{Fc}](\frac{2}{3}[\text{Fc}])^{3/2}))$$

$$\text{And } \Delta E = RT/nF * (2\ln([\text{Fc}^+]/[\text{Fc}]^{4/5}) - 3/2\ln(2/3))$$

Knowing that $n = 1$ and $T = 293 \text{ K}$, and inserting the above cell potentials (as $E_{p/2}$ values) in order to estimate ΔE , this allows us to estimate the resulting ferrocene:ferrocenium ratios at equilibrium when 1.5 equivalents of iodine have been added. For the three investigated systems, these are

Dibutanoylferrocene : dibutanoylferrocenium = 90 : 10

Ferrocene : Ferrocenium = 1 : 99

Dibutylferrocene : Dibutylferrocenium = 0.1 : 99.9

It should be noted that these are theoretical estimates for the situation at 293 K, and from measurements of the two components in isolation from each other. The reality of the mixed compounds is somewhat more complicated, as demonstrated below and in Fig. 3 of the manuscript. As the ΔE values decreased by (crudely) 100 mV in each case, each system is slightly closer to a 50:50 mixture than the values expressed above.

4. Cyclic voltammetry of the ferrocenium triiodide compounds

Cyclic voltammetry was recorded in [Emim][NTf₂] for the ferrocene compounds by themselves, iodine, and the same solutions when mixed. The current response from the CVs of just ferrocene and just iodine were summed, in order to compare with the response of the

mixture (ferrocenium triiodide). Significant discrepancy indicates ‘nonadditivity’ of the faradaic current, whereby more or less current is observed than can be expected based upon the known material present.

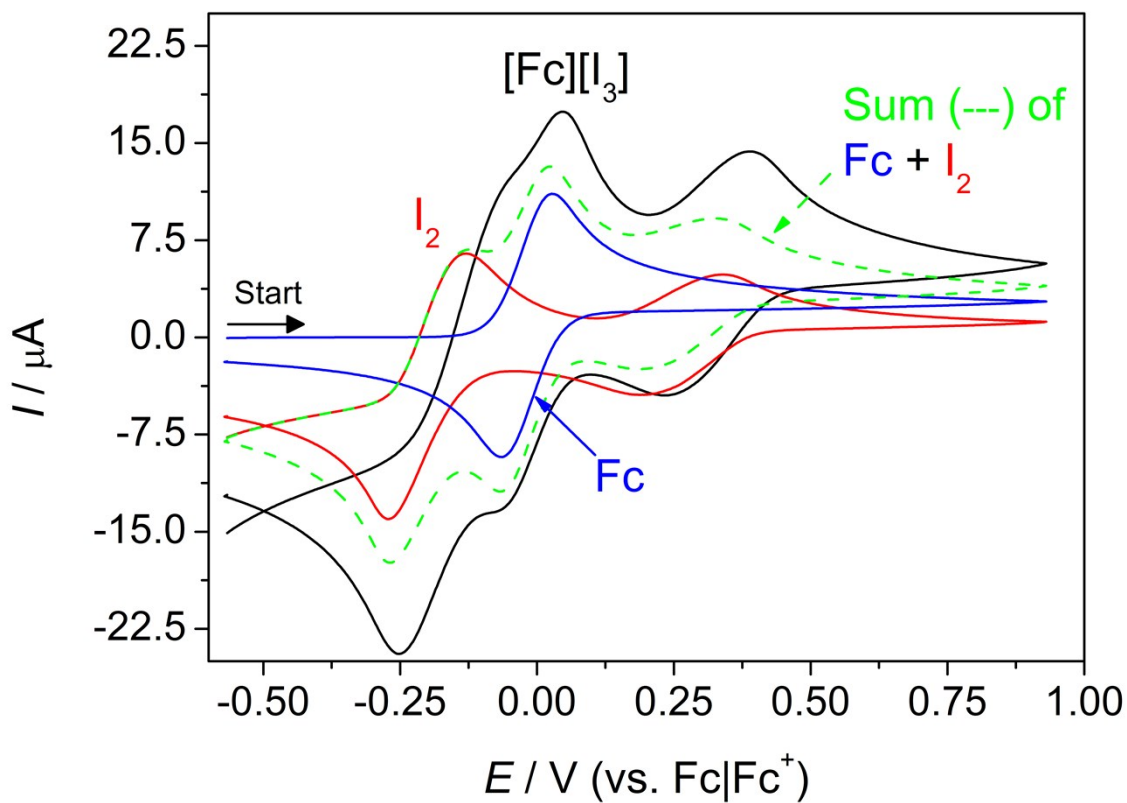


Fig. S7: CVs recorded for 15 mM **Fc**, 22.5 mM **I₂**, the additive **sum** of these two scans, and 15 mM **[Fc][I₃]**. All in **[Emim][NTf₂]**. Scans recorded at a 1.6 mm Pt electrode, 50 mV s^{-1} , at 293 K, and corrected to the $\text{Fc} | \text{Fc}^+$ formal potential.

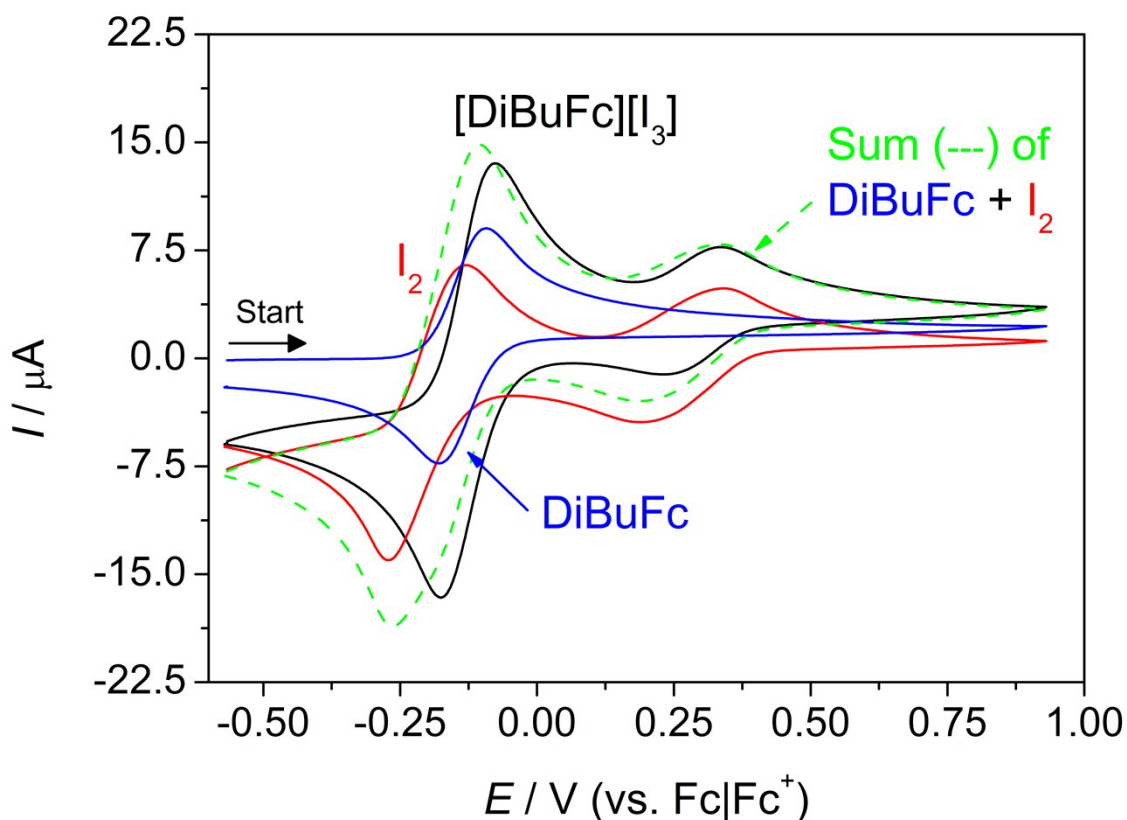


Fig. S8: CVs recorded for 15 mM **DiBuFc**, 22.5 mM **I₂**, the additive **sum** of these two scans, and 15 mM **[DiBuFc][I₃]**. All in **[Emim][NTf₂]**. Scans recorded at a 1.6 mm Pt electrode, 50 mV s⁻¹, at 293 K, and corrected to the Fc | Fc⁺ formal potential.

References

1. (a) M. D. Vukićević, Z. R. Ratković, A. V. Teodorović, G. S. Stojanović and R. D. Vukićević, *Tetrahedron*, 2002, **58**, 9001-9006; (b) M. Vogel, M. Rausch and H. Rosenberg, *The Journal of Organic Chemistry*, 1957, **22**, 1016-1018.
2. L. Barote, R. Weissbach, R. Teodorescu, C. Marinescu and M. Cirstea, 2008.
3. S. I. Goldberg, W. D. Bailey and M. L. McGregor, *The Journal of Organic Chemistry*, 1971, **36**, 761-769.
4. M. S. Romano, N. Li, D. Antiohos, J. M. Razal, A. Nattestad, S. Beirne, S. Fang, Y. Chen, R. Jalili, G. G. Wallace, R. Baughman and J. Chen, *Advanced Materials*, 2013, **25**, 6602-6606.
5. (a) T. Hirai, K. Shindo and T. Ogata, *Journal of The Electrochemical Society*, 1996, **143**, 1305-1313; (b) T. I. Quickenden and C. F. Vernon, *Solar Energy*, 1986, **36**, 63-72.
6. (a) R. Hu, B. A. Cola, N. Haram, J. N. Barisci, S. Lee, S. Stoughton, G. Wallace, C. Too, M. Thomas, A. Gestos, M. E. Cruz, J. P. Ferraris, A. A. Zakhidov and R. H. Baughman, *Nano*

- Letters*, 2010, **10**, 838-846; (b) H. A. H. Alzahrani, J. J. Black, D. Goonetilleke, J. Panchompoo and L. Aldous, *Electrochemistry Communications*, 2015, **58**, 76-79.
7. N. G. Connelly and W. E. Geiger, *Chemical Reviews*, 1996, **96**, 877-910.